Acta Mechanica 173, 13–17 (2004)
DOI 10.1007/s00707-004-0174-2

Acta Mechanica
Printed in Austria

Shear horizontal vibrations of a piezoelectric/ferroelectric wedge

J. S. Yang, Lincoln, Nebraska

Received May 6, 2004; revised August 23, 2004
Published online: November 8, 2004

Summary. An exact solution is obtained for shear horizontal vibrations of a piezoelectric wedge of polarized ceramics. The results are useful for understanding and accurately predicting energy trapping of shear horizontal modes in resonant piezoelectric devices.

1 Introduction

Shear horizontal vibration modes of plates (including face-shear and thickness-twist modes) are often used for bulk acoustic wave piezoelectric resonators and other devices [1]. An important behavior of these modes is the energy trapping phenomenon [2] by which shear vibrations of a plate can be confined to be near the center of the plate. Near the edge of the plate there is essentially no vibration so that wiring and mounting near the edge do not affect the vibration. Energy trapping may be due to the mass effect of electrodes [2]. Contoured plates with varying thickness have been used to achieve stronger energy trapping [3]. Due to the wide use of contoured plate resonators, the study of energy trapping in these resonators has been of continuing research interest, e.g., [3]–[10]. Quartz is the most widely used material for piezoelectric resonators. Since piezoelectric coupling is very weak in quartz, in the analyses of energy trapping in quartz usually the small piezoelectric coupling is neglected and an elastic analysis is performed [2]–[5], [7]. Recently, new piezoelectric crystals of the langasite family have been developed for resonator applications [11]. These new crystals have relatively strong piezoelectric coupling which should be included in the analysis. Polarized ceramics also have strong piezoelectric coupling and are often used for piezoelectric devices operating with shear modes with energy trapping [12]. Since contoured resonators lead to differential equations with variable coefficients when two-dimensional structural equations for plates are used, all the modeling work known to the author involves approximations due to the use of two-dimensional plate equations. Sometimes additional approximations are introduced because of the use of methods like perturbation etc.

In this paper, we show that exact solutions can be obtained for a piezoelectric ceramic wedge in shear horizontal vibrations. Since a wedge is often used in contoured resonators for energy trapping, the results obtained are of fundamental importance to the understanding and design of contoured piezoelectric resonators.

2 Governing equations

Consider a semi-infinite wedge of ceramics poled in the x_3-direction as shown in Fig. 1. The wedge is unbounded in the x_3-direction. For device applications we consider the case that the wedge surfaces are traction-free and are unelectroded. Effects of the electric field that may exist in the surrounding free space are known to be small and are neglected as usual [3]–[10]. We are interested in anti-plane motion [13] with

$$u_1 = u_2 = 0, \quad u_3 = u_3(x_1, x_2, t), \quad \phi = \phi(x_1, x_2, t). \tag{1}$$

The non-vanishing strain and electric field components are

$$\begin{Bmatrix} 2S_{13} \\ 2S_{23} \end{Bmatrix} = \nabla u, \quad \begin{Bmatrix} E_1 \\ E_2 \end{Bmatrix} = -\nabla \phi, \tag{2}$$

where $\nabla = \mathbf{i}_1 \partial_1 + \mathbf{i}_2 \partial_2$ is the two-dimensional gradient operator. The nontrivial components of T_{ij} and D_i are

$$\begin{Bmatrix} T_{13} \\ T_{23} \end{Bmatrix} = c\nabla u + e\nabla \phi, \quad \begin{Bmatrix} D_1 \\ D_2 \end{Bmatrix} = e\nabla u - \varepsilon \nabla \phi, \tag{3}$$

where we have denoted $c = c_{44}, e = e_{15}$, and $\varepsilon = \varepsilon_{11}$. The nontrivial equation of motion and the charge equation of electrostatics take the following form:

$$c\nabla^2 u + e\nabla^2 \phi = \rho u_{,tt},\ e\nabla^2 u - \varepsilon \nabla^2 \phi = 0, \tag{4}$$

where $\nabla^2 = \partial_1^2 + \partial_2^2$ is the two-dimensional Laplacian. We introduce [13]

$$\psi = \phi - \frac{e}{\varepsilon} u, \tag{5}$$

then

$$\begin{aligned} &T_{23} = \bar{c} u_{3,2} + e\psi_{,2}, \quad T_{31} = \bar{c} u_{3,1} + e\psi_{,1}, \\ &D_1 = -\varepsilon \psi_{,1}, \quad D_2 = -\varepsilon \psi_{,2}, \end{aligned} \tag{6}$$

and

$$v_T^2 \nabla^2 u = u_{,tt}, \quad \nabla^2 \psi = 0, \tag{7}$$

where

$$v_T^2 = \frac{\bar{c}}{\rho}, \quad \bar{c} = c + \frac{e^2}{\varepsilon} = c(1 + k^2), \quad k^2 = \frac{e^2}{\varepsilon c}. \tag{8}$$

3 An exact solution

In polar coordinates defined by $x_1 = r\cos\theta$ and $x_2 = r\sin\theta$, Eq. (7) takes the form

$$v_T^2 \left(\frac{\partial^2 u}{\partial r^2} + \frac{1}{r}\frac{\partial u}{\partial r} + \frac{1}{r^2}\frac{\partial^2 u}{\partial \theta^2}\right) = u_{,tt} \quad \frac{\partial^2 \psi}{\partial r^2} + \frac{1}{r}\frac{\partial \psi}{\partial r} + \frac{1}{r^2}\frac{\partial^2 \psi}{\partial \theta^2} = 0. \tag{9}$$

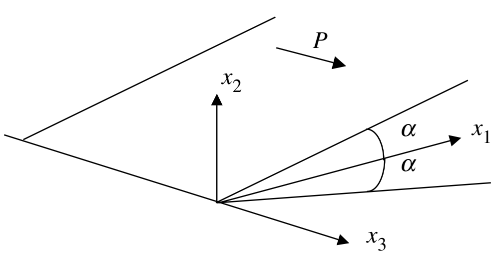

Fig. 1. A piezoelectric wedge of polarized ceramics and coordinate system

Consider the possibility of the following fields which are odd in θ and may be called anti-symmetric modes:

$$u(r,\theta,t) = u(r)\sin v\theta \exp(-i\omega t), \quad \psi(r,\theta,t) = \psi(r)\sin v\theta \exp(-i\omega t). \tag{10}$$

Substitution of Eq. (10) into Eq. (9) results in

$$\frac{\partial^2 u}{\partial r^2} + \frac{1}{r}\frac{\partial u}{\partial r} + (\xi^2 - \frac{v^2}{r^2})u = 0, \quad \frac{\partial^2 \psi}{\partial r^2} + \frac{1}{r}\frac{\partial \psi}{\partial r} - \frac{v^2}{r^2}\psi = 0, \tag{11.1,2}$$

where we have denoted

$$\xi = \frac{\omega}{v_T}. \tag{12}$$

ξ may be viewed as a wave number in the r-direction. Equation (11.1) can be written as Bessel's equations of order v. Equation (11.2) allows a simpler power function solution. The general solutions can be written as

$$\begin{aligned} u &= [C_1 J_v(\xi r) + C_2 Y_v(\xi r)]\sin v\theta \exp(-i\omega t), \\ \psi &= [C_3 r^v + C_4 r^{-v}]\sin v\theta \exp(-i\omega t), \end{aligned} \tag{13}$$

where J_v and Y_v are the v-th order Bessel functions of the first and second kind. C_1–C_4 are undetermined constants. Since Y_v and r^{-v} are singular at the origin, terms associated with C_2 and C_4 have to be dropped. From Eq. (6) the stress and electric displacement components needed for boundary conditions can be obtained. Hence

$$\begin{aligned} u &= C_1 J_v(\xi r)\sin v\theta \exp(-i\omega t), \\ \psi &= C_3 r^v \sin v\theta \exp(-i\omega t), \\ T_{\theta z} &= [\bar{c}\frac{v}{r}C_1 J_v(\xi r) + e\frac{v}{r}C_3 r^v]\cos v\theta \exp(-i\omega t), \\ D_\theta &= -\varepsilon\frac{v}{r}C_3 r^v \cos v\theta \exp(-i\omega t). \end{aligned} \tag{14}$$

At $\theta = \pm\alpha$ we need to impose the following boundary conditions for a free wedge:

$$\begin{aligned} T_{\theta z} &= [\bar{c}\frac{v}{r}C_1 J_v(\xi r) + e\frac{v}{r}C_3 r^v]\cos v\alpha \exp(-i\omega t) = 0, \\ D_\theta &= -\varepsilon\frac{v}{r}C_3 r^v \cos v\alpha \exp(-i\omega t) = 0, \end{aligned} \tag{15}$$

which implies that

$$\cos v\alpha = 0, v = \frac{n\pi}{2\alpha}, n = 1,3,5,\ldots\ . \tag{16}$$

Equation (16) determines the order of the Bessel function.

In a similar way, if the sin $v\theta$ factor in Eq. (10) is replaced by cos $v\theta$, a set of symmetric modes is obtained:

$$\begin{aligned} u &= C_1 J_v(\xi r)\cos v\theta \exp(-i\omega t), \\ \psi &= C_3 r^v \cos v\theta \exp(-i\omega t), \\ v &= \frac{n\pi}{2\alpha}, n = 0,2,4,6,\ldots\ . \end{aligned} \tag{17}$$

4 Discussion

Note that in the modes given by Eq. (14) and Eq. (17) ψ is unbounded for large r. If we require boundedness of ψ at lager r, C_3 must vanish. Then $\psi = 0$, and from Eq. (5) the electric potential is given by

$$\phi = \begin{cases} \frac{e}{\varepsilon} C_1 J_v(\xi r) \sin v\theta \exp(-i\omega t), n = 1, 3, 5, \ldots, \\ \frac{e}{\varepsilon} C_1 J_v(\xi r) \cos v\theta \exp(-i\omega t), n = 0, 2, 4, \ldots \ . \end{cases} \tag{18}$$

Since a wedge occupies a semi-infinite region, we have a continuous spectrum. For any given ω, a ξ can be determined from Eq. (12). Then anti-symmetric and symmetric modes are given by (14) and (17), respectively.

For resonator applications, we are interested in long waves in a narrow wedge with a small α. For a narrow wedge, from Eq. (16), v is large. We have Bessel functions with large orders. By long waves we mean that, at a finite r, the wavelength λ is much larger than the local wedge thickness:

$$\lambda = \frac{2\pi}{\xi} >> 2\alpha r, \quad \text{or} \quad \xi r << \frac{\pi}{\alpha}. \tag{19}$$

In this case ξr has to be small or no more than being finite.

For the lowest symmetric mode with $n = 0$ (face-shear), from Eq. (17) $v = 0$ irrespective of what α is. Since $J_0(0) = 1$, the tip of the wedge is vibrating and this mode is not trapped.

All other modes ($n = 1, 2, 3, 4, \ldots$), symmetric or anti-symmetric, may be called thickness-twist modes. For these modes v is positive. For small arguments, Bessel functions have the following asymptotic expression:

$$J_v(x) \cong \frac{x^v}{2^v \Gamma(1 + v)}, \tag{20}$$

which shows that $J_v(0) = 0$ and the modes grow from the tip of the wedge. Therefore all thickness-twist modes show energy trapping because they vanish at the wedge tip and grow away from there. The growing rate is small for a large v, or a small α. Since Bessel functions decay to zero for large arguments, trapped mode vanishes both at the wedge tip and at infinity when C_3 is taken to be zero.

The above observations are based on the displacement field. It is also informative to examine the stress, strain, electric field and electric displacement fields. For a general measure of all fields we consider the internal energy density. For example, for the anti-symmetric modes in Eq. (14), from the real parts of the fields, we obtain the internal energy density as

$$U = \frac{1}{2} \bar{c} C_1^2 \left\{ \xi^2 \left[J_v'(\xi r) \right]^2 \sin^2 v\theta + \frac{v^2}{r^2} J_v^2(\xi r) \cos^2 v\theta \right\} \cos^2 \omega t. \tag{21}$$

Equation (21) shows that although the displacement vanishes at the wedge tip for any $v > 0$, the internal energy density vanishes at the wedge tip only when $v > 1$. This is not surprising in view of the fact that the energy density depends on the displacement gradient.

Bessel functions are well tabulated and plotted. Readers who are interested in further details may find them in many references, e.g., [14] and the references therein. The purpose of this paper is to show that a set of exact shear horizontal modes in a ceramic wedge can be obtained in terms of these functions.

5 Conclusions

A set of exact piezoelectric shear horizontal modes is obtained for a ceramic wedge. Face shear modes in a wedge are not trapped, but all thickness-twist modes are. The solution is useful for the understanding and accurate prediction of energy trapping in piezoelectric devices. They can also be used as a benchmark for the continuing study on energy trapping in piezoelectric devices by approximate or numerical methods.

Acknowledgement

This work was supported by the US Army Research Office under DAAD19-01-1-0443.

References

[1] Mindlin, R. D.: An introduction to the mathematical theory of vibrations of elastic plates. Fort Monmouth, NJ: U.S. Army Signal Corps Engineering Laboratories 1955.
[2] Mindlin, R. D., Lee, P. C. Y.: Thickness-shear and flexural vibrations of partially plated, crystal plates. Int. J. Solids Struct. **2**, 125–139 (1966).
[3] Mindlin, R. D., Forray, M.: Thickness-shear and flexural vibrations of contoured crystal plates. J. Appl. Phys. **25**, 12–20 (1954).
[4] Bleustein, J. L.: Thickness-twist and face-shear vibrations of a contoured crystal plate. Int. J. Solids Struct. **2**, 351–360 (1966).
[5] Lee, P. C. Y., Chen, S.-S.: Vibrations of contoured and partially plated, contoured, rectangular AT-cut quartz plates. J. Acoust. Soc. Am. **46**, 1193–1202 (1969).
[6] Stevens, D. S., Tiersten, H. F.: An analysis of doubly rotated quartz resonators using essentially thickness modes with transverse variation. J Acoust. Soc. Am. **79**, 1811–1826 (1986).
[7] Yang, J. S.: The vibration of a circular plate with varying thickness. J. Sound Vibr. **165**, 178–184 (1993).
[8] Yang, J. S., Tiersten, H. F.: An analysis of contoured quartz resonators with beveled cylindrical edges. In: Proc. IEEE Frequency Control Symp., pp. 727–739, IEEE 1995.
[9] Lee, P. C. Y., Wang, J.: Piezoelectrically forced thickness-shear and flexural vibrations of contoured quartz resonators. J. Appl. Phys. **79**, 3411–3422 (1996).
[10] Wang, J.: Thickness-shear and flexural vibrations of linearly contoured crystal strips with multiprecision computation. Comp. Struct. **70**, 437–445 (1999).
[11] Smythe, R. C., Helmbold, R. C., Hague, G. E., Snow, K. A.: Langasite, langanite, and langatate bulk-wave Y-cut resonators. IEEE Trans. Ultrasonics, Ferroelectrics, and Frequency Control **47**, 355–360 (2000).
[12] Abe, H., Yoshida, T., Watanabe, H.: Energy trapping of thickness-shear vibrations excited by parallel electric field and its applications to piezoelectric vibratory gyroscopes. In: Proc. IEEE Int. Ultrasonics Symp., pp. 467–471, IEEE 1998.
[13] Bleustein, J. L.: A new surface wave in piezoelectric materials. Appl. Phys. Lett. **13**, 412–413 (1968).
[14] Whittaker, E. T., Watson, G. N.: A course of modern analysis. London: Cambridge University Press 1965.

Author's address: J. S. Yang, Department of Engineering Mechanics, University of Nebraska, Lincoln, NE 68588-0526, U.S.A. (E-mail: jyang1@unl.edu)